ISSN 0018-151X, High Temperature, 2017, Vol. 55, No. 2, pp. 263–272. © Pleiades Publishing, Ltd., 2017.
Original Russian Text © K.A. Vereshchagin, D.N. Kozlov, V.V. Smirnov, O.M. Stel'makh, V.I. Fabelinsky, 2017, published in Teplofizika Vysokikh Temperatur, 2017, Vol. 55, No. 2, pp. 273–283.

HEAT AND MASS TRANSFER AND PHYSICAL GASDYNAMICS

Measurements of Temperature Spatial Distribution and Fluctuations in a Hydrogen-Oxygen Flame at High Pressures by Means of Coherent Anti-Stokes Raman Spectroscopy

K. A. Vereshchagin, D. N. Kozlov, V. V. Smirnov, O. M. Stel'makh, and V. I. Fabelinsky*

Prokhorov General Physics Institute, Russian Academy of Sciences,
Moscow 119991, Russia
**e-mail: vif@kapella.gpi.ru*

Received March 2, 2015

Abstract—The results of measurements of the temperature field in a hydrogen-oxygen flame by means of broadband coherent anti-Stokes Raman spectroscopy are presented. The measurements were performed at pressures up to 1.7 MPa and temperatures ~3000 K with the spatial resolution of ~0.04 × 0.04 × 2.5 mm^3. The duration of a single measurement was 10 ns and the sampling rate was 10 Hz. The error of the temperature determination was ~4% for the single-shot measurements and ~0.15% for the measurements of the average values during 100 s under quasi-stationary burning conditions.

DOI: 10.1134/S0018151X17010230

INTRODUCTION

Local non-intrusive optical diagnostics of the gas medium during a combustion process is a powerful method of investigation and diagnostics, which is applied in the leading aerospace corporations when developing modern aircraft and rocket engines employing gaseous and cryogenic hydrogen-oxygen (H_2/O_2), methane-oxygen (CH_4/O_2), or kerosene-oxygen combustible mixtures. Turbulent component mixing [1], and high temperatures (~3000 K) and pressures (~10 MPa) of the gas medium in the combustion chamber, necessary to enhance their energy efficiency [2], are the characteristic features of operation of these engines.

In the view of optimization of combustion chamber design, of particular interest are the measurements of gas temperature and number densities of the molecular mixture components in different spatial points of the flame, of temporal fluctuations of these parameters and their dependence on the fuel and oxidizer mass flow rates and on the pressure in the combustion chamber. Knowledge of the spatial distributions of the combustion process parameters is necessary to characterize the combustion chamber, to study the combustion process itself and the combustion efficiency, as well as to verify the process theoretical calculation models and the engineering approaches to combustion chamber and nozzle unit design.

Spectroscopic methods provide non-intrusive and non-invasive combustion diagnostics employing the shape and relative line intensities of the probe molecule spectra. Here, in contrast to the methods of linear spectroscopy (see [3] for example), the methods of nonlinear laser spectroscopy [4] make it possible to determine gas mixture temperature and composition with high spatial (~1 mm) and temporal (~10 ns) resolution. Besides, application of these methods provides information on the degree of thermodynamic non-equilibrium between the vibrational and the rotational degrees of freedom of gas molecules in the combustion chambers. Local temperature fluctuation measurements in the quasi-stationary burning conditions turn to be also possible by means of the pulse-repetitive registration of single-shot spectra at a high rate (10–100 Hz). In particular, in hydrogen-oxygen combustion, simultaneous determination, in one and the same spatial point, of H_2 and H_2O vapor concentrations or, at least, their ratio makes it possible to control the fluctuations of the combustion efficiency. Since the measurements should be performed in different flame zones, as well as under different mass flow rates of the initial components and gas pressures, which provide the variations of local mixture composition, even if the task is only limited to thermometry, the demand appears to use the spectra of different probe molecules, e.g., H_2 and H_2O, for temperature determination. On the other hand, registration of spectra of several molecules enables to obtain complementary information and increases the measurement accuracy. Application of nonlinear laser spectroscopy is especially essential in the cases when the use of the traditional methods of non-invasive optical thermometry (e.g., pyrometry) is in fact impossible, and one has to rely only on the results of calculations.

Spectroscopy of coherent anti-Stokes Raman scattering (CARS) [5] is a widely acknowledged highly sensitive non-intrusive method of local measurements of gas mixture temperature and composition. When measuring by this technique, radiation from two (or three), usually pulsed, lasers is directed into the medium. As a rule, the lasers have the pulse energy of about 1–100 mJ, the pulse duration within the range of 1–10 ns, and the pulse repetition rate from a few to tens of Hz. The emission frequency of one of the lasers, ν_L, is fixed and the spectral line width, $\Delta\nu_L$, is low whereas the frequency of the other one, ν_S, can either be tuned (having a small width $\Delta\nu_S$) or be fixed but, in that case, the emission line width $\Delta\nu_S$ is large enough to enable simultaneous registration of several resonances. Due to nonlinear mixing caused by the third-order susceptibility of the medium, the radiation of the two high-power pump lasers generates the anti-Stokes radiation at the frequency $\nu_A = 2\nu_L - \nu_S$, The power of this radiation undergoes the resonance increase when the frequency difference $\nu_L - \nu_S$ approaches a frequency ν_0 of a Raman-active transition of a molecular component of the medium. If the laser line width at the Stokes frequency ν_S is narrow, then the spectral information is obtained by means of measuring the emission power at the ν_A frequency in dependence on the tunable frequency ν_S (the so-called "narrowband CARS spectroscopy with the tunable pump"). In the case when the laser line width at the ν_S frequency is broad (this version is called "broadband CARS spectroscopy"), the information on the medium is obtained from the anti-Stokes emission spectrum with the frequencies close to ν_A. This emission is dispersed by a spectral instrument and registered by a multichannel photodetector.

To increase CARS signal strength, which nonlinearly depends on the pump intensity, the laser beams are usually focused into the probe volume. Here, the anti-Stokes radiation is generated within a small zone of intersection of the interacting focused laser beams thus providing the high spatial resolution of the measurements. Then, the high temporal resolution of a spectrum registration during a single laser shot is defined by the pump laser pulse duration, and the data output rate – by the repetition rate of the laser pulses. The physical basis of CARS spectroscopy, as well as the principles and the peculiarities of its application are described in detail in the reviews [5–8].

Previously, in [9], we applied "dual-broadband CARS"[1] [10–15] and showed that, in the case of diffusion combustion of H_2/O_2 mixture at the atmospheric pressure, CARS spectroscopy of rovibrational transitions of H_2 molecules used as a probe makes it possible to successfully implement local measurements of temperature and H_2 molecule number density in the flame. The application of dual-broadband CARS made it possible to achieve the accuracy of "instantaneous", single-shot temperature measurements of about 4–5% within the range of 2000–3000 K [9]. As the laboratory test object, a rather stable flame of a small open axis-symmetric burner, with continuous oxidizer and fuel supply through the central hole and the surrounding concentric slit, respectively, was employed in [9].

The aim of the present work is to study the possibilities to apply dual broadband CARS spectroscopy for the measurements of temperature spatial distributions in the medium during combustion of H_2/O_2 mixtures in a continuous high-pressure turbulent flow. The measurements were performed inside an enclosed volume of a continuous high-pressure laboratory burner, in which the temperature and the pressure were close to those characteristic for engine combustion chambers. The burner was operating at pressures up to 2.6 MPa, and the combustion, in contrast to the atmospheric pressure case, was significantly unstable. The local temperature values were determined from H_2 molecule CARS spectra, both time-averaged and registered in a single laser shot.

EXPERIMENT

In our measurements, the CARS spectrometer similar to that described in [9] was used. Its layout is shown in Figure 1. The laser part of the spectrometer consisted of the three lasers: the *Q*-switched Nd^{3+}:YAG-laser (DCR-3D, Quanta Ray), PL, providing the second harmonics ($\lambda_L = 532$ nm) emission pulses with the energy of about 150 mJ, the repetition rate of 10 Hz, the duration of 10 ns, the spectral width[2] of 0.7 cm^{-1}, and the intermode spacing of 0.005 cm^{-1}; and the two dye lasers, each consisting of an oscillator-amplifier pair, with the broad output emission spectrum. A part of the 532 nm emission (~20–30 mJ) was engaged in the four-wave mixing in the CARS process itself and the rest was used to pump the dye cells of the dye lasers. All the pump emissions had the same (vertical) polarization.

The dye laser, DL1, with the amplifier, A1 (see Fig. 1), operated with a Rhodamine 6G/methanol solution at the wavelength of $\lambda_{L1} = 553$ nm, and had the spectral width at half-maximum (FWHM) $\Delta\nu_{L1} \sim 170$ cm^{-1} and the pulse energy of about 3 mJ. In case of the dual broadband pumping of H_2 molecule transitions, the dye laser, DL2, with the amplifier, A2, operated with a

[1] "Dual-broadband CARS" is a more complicated version of CARS at broadband pumping where three different lasers are employed, two of them having a broadband spectrum. The advantage of this version is the higher accuracy of measurement of the amplitudes in the registered anti-Stokes emission spectrum.

[2] "Inverse centimeter" (cm^{-1}) is the customary off-system measurement unit in the spectroscopy; its physical meaning is frequency; its typical numerical values are "handy": ν [cm^{-1}] = ν [Hz]/c[cm/s] where c is the light velocity in vacuum.

Pyridine 1/dimethylsulfoxide (DMSO) solution ($\lambda_{L2} = 713$ nm, $\Delta\nu_{L2} \sim 350$ cm^{-1}, 1.5 mJ). The difference between the central frequencies of the two dye lasers (~4000 cm^{-1}) corresponds to the transition frequency range of the $\upsilon = 0 \rightarrow \upsilon = 1$ Q-branch band (^{0-1}Q-branch) of H_2 molecules, that is, 3780–4170 cm^{-1}.

In case of broadband CARS spectroscopy of H_2O molecules, we used only the DL2-A2 dye laser with a DCM/DMSO solution ($\lambda_L = 660$ nm, $\Delta\nu_L \sim 300$ cm^{-1}, 8 mJ). The difference in the pump laser frequencies (~3600 cm^{-1}) corresponds to the frequencies of the $\upsilon = 0 \rightarrow \upsilon = 1$ Q-branch band of the $\nu_1 = 3652$ cm^{-1} mode of the H_2O molecule spectrum (3400–3700 cm^{-1}).

The unstable cavity Nd^{3+}:YAG-laser had a donut-like intensity profile and the pump beams were crossed in a so-called USED-CARS configuration [11]: the dye laser beams pass through the center of the hole in the donut-like Nd^{3+}:YAG-laser profile and are focused into the probe volume by the lens, L_1 ($f = 300$ mm). The laser beam waist diameter in the lens focus was ~0.04 mm and the length of generation of more than 90% of the CARS pulse energy was equal to 2.5 mm – these two values defined the transversal and the longitudinal spatial resolutions, respectively.

After the collimation of the beams passing through the chamber of the burner, HPB, by the lens, L_2 ($f = 300$ mm), we separated the desired anti-Stokes emission by means of the dichroic mirror and of the holographic bandpass filter, F, and focused it by the converging lens, L_3 ($f = 20$ mm), into the fused silica fiber, OF (400 μm in diameter, 6 m long), to transfer to the spectrograph, GS, located outside the room where the high pressure burner operates. In order to match the beam divergence with the numerical aperture of the spectrograph and to form an image of the output fiber endface on the entrance slit of the spectrograph we used the telescope, T. It was located between the output fiber end and the spectrograph. Total transmission coefficient of the fiber and the relay optics was about 10–15%.

The CARS emission spectrum dispersed by the HR1000 (Jobin-Yvon) spectrograph with the focal length of 1 m and the 2400 grooves/mm holographic grating was registered by the IRY 1024 (Spectroscopy Instruments) linear multichannel photodetector, MCD, equipped with a gated image intensifier. Full width of the spectrograph slit function (at the half-maximum) was about 3 cm^{-1}, thus making it possible to resolve all the narrow vibrational-rotational lines present in the ^{0-1}Q-branch of the H_2 CARS spectrum. Note that their width, under all conditions, was defined by the slit function width. We recorded CARS signals either as a single spectrum accumulated for 100–1000 laser shots or as a series of 300 or 1000 single shot spectra following each other at the repetition rate of 10 Hz.

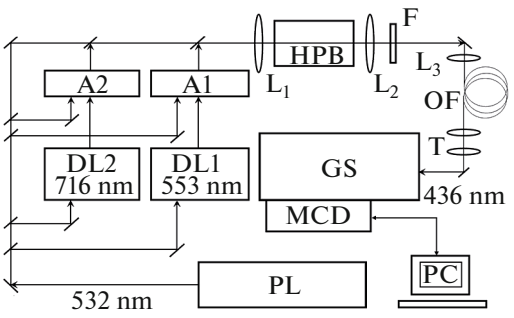

Fig. 1. Layout of the experimental set-up for dual-broadband CARS spectroscopy.

The laboratory burner where we investigated the continuous burning of the H_2/O_2 mixture was located in the high pressure stainless steel chamber with the optical windows. The chamber was mounted on the table with the three-dimensional translation stages. The fuel and the oxidizer were continuously fed into the chamber via the injection unit installed at the water cooled copper plate in the lower part of the chamber. We used the two types of injection units. The first one was the single coaxial injector with the central hole, 1.7 mm in diameter (to feed O_2) and the surrounding slit, 2.5 mm in inner diameter, 0.2 mm wide (to feed H_2). The second one comprised 35 coaxial injectors each with the central hole, 0.5 mm in diameter (to feed O_2) and the surrounding slit, 0.8 mm in inner diameter, 0.2 mm wide (to feed H_2). These 35 injectors were assembled in a hexagonal matrix with the characteristic transversal dimension of 10 mm. The main principle of such an injector operation is as follows: the components enter the combustion zone as the separate coaxial jets thus preventing their preliminary mixing, and the vortices occurring in the boundary layers of those jets provide efficient mixing of the fuel and the oxidizer. Those vortices cause the flame turbulence. In our case, the typical Reynolds number range for the jets was equal $(3–10) \times 10^3$. The desired mixture composition was maintained by means of the mass flow rate controllers (EL-FLOW F-232C, Bronkhorst) in the gas supply system. The mixture stoichiometry, Φ, was determined as the ratio of the established mass flow rates of the fuel and the oxidizer normalized by their stoichiometric ratio. The required operation pressure inside the chamber was maintained by means of its additional pressure boost by the buffer gas (N_2) flow over the flame periphery while using the throttle installed at the chamber output.

Adding of the buffer gas resulted, due to its turbulent mixing with hydrogen and oxygen and of its diffusion into the torch section, in the combustible mixture dilution and in the respective variations of the flame parameters – the flame geometry variation and its shortening and shift to the plate with the injectors – under the chamber pressure increase. For example,

when using the single injector, the characteristic visible torch size along the vertical burner axis reached 50–60 mm at 0.1 MPa and decreased to 25–30 mm at 1.7 MPa; here, the torch diameter in the widest part increased from ~10 mm to ~15 mm.

At the increased pressures, convective flows occurred inside the chamber and the flame began to lose its stability. This caused, along with the pump beam refraction effects, essential intensity fluctuations of the anti-Stokes emission from one shot to another. The experiments showed that, in the given burner, reliable measurements near the injector plate might be only performed at the pressures below 2.6 MPa.

The influence of the beam refraction inside the chamber on the efficiency of the anti-Stokes emission coupling to the fiber, due to the image shift at its input face, was experimentally verified at different pressures. For this purpose, the attenuated beam of a He-Ne laser passing through the flame, and a high resolution TV-camera CCD-matrix, with the known spacing between the pixels, were used. It turned out that, up to the pressures ~1.7 MPa, the image shifts are insufficient whereas, at the pressures about 2.6 MPa, these shifts cause noticeable fluctuations of the shot-to-shot signal intensity.

CALIBRATION MEASUREMENTS AND THE ALGORITHM OF THE TEMPERATURE DETERMINATION FROM THE H_2 SPECTRA

The high-temperature calibration measurements based on the H_2 ^{0-1}Q-branch dual broadband CARS spectra were performed in [12–15] in the McKenna burner flame at temperatures of 1400–1900 K under stationary and well-controlled conditions of combustion of the premixed H_2/air mixture at atmospheric pressure. The main target of our calibration measurements, based on the H_2 CARS spectra, carried out in the similar burner and presented in [9], was to test the engaged CARS spectrometer and to verify the data processing software, as well as to estimate the obtained accuracy of the temperature determination in a single laser shot. To facilitate the direct comparison of our results with those presented in [12, 15], we performed all the temperature measurements in that very flame point and at those very conditions.

In [9], we determined the temperature from the H_2 spectra by means of relatively simple procedure using the integral intensities, I_J, of the single, most intense rotational components of the H_2 ^{0-1}Q-branch spectrum with the odd rotational quantum numbers, J, instead of calculations and fitting the whole spectral profile (e.g., [13]). We did not take into account the intensities of the "hot" band, $\upsilon = 1 \to \upsilon = 2$ (^{1-2}Q-branch), lines, even if observed in the spectra. Within a wide pressure range, CARS spectra of H_2 in the combustion zone look like a set of narrow and isolated lines with the same width determined by the slit function of the spectrometer detection system (about 3 cm^{-1}). Sometimes, these lines may be located on the unstructured nonresonant background with its relative intensity depending on the local medium composition. As far as the typical full widths of the CARS spectrum and of the broadband pump laser spectrum are comparable, the spectral distribution of the laser intensity perturbs the CARS spectrum shape. To take into account this perturbance, we registered the averaged nonresonant CARS spectra in the air at the beginning and at the end of registration of each series of the single-shot spectra. We integrated the intensity of each rotational component after normalization of the resonant spectrum by the averaged nonresonant one, and then subtracted the nonresonant background within the interval of about two–three full line widths close to the line center location. Thus obtained values of the integral line intensities, I_J, under neglecting the neighboring line wings contributions, can be represented by the relation

$$I_J = \mathrm{const} a_J^2 S(\Gamma_J), \tag{1}$$

with the a_J coefficient equals to

$$a_J = \frac{Nc^4}{\hbar(2\pi\nu_{S2})^4}\Delta\rho_J\left(\frac{d\sigma}{d\Omega}\right)_J, \tag{2}$$

where N is the number density of the registered gas molecules; $\hbar$ and c are the Plank constant and the speed of light, respectively; $\Delta\rho_J$ is the depending on the temperature and normalized by the density, N, population difference of the levels connected by the given J-th Raman-active transition with the frequency of ν_J; $(d\sigma/d\Omega)_J$ and Γ_J are the Raman cross-section and the Lorentzian collisional line width (half-width at half-maximum, HWHM), respectively, for the given molecular transition; the $S(\Gamma_J)$ value is the spectral overlap integral [16] for the particular lines. In (2), we account for the contribution into the integral line intensities of the weak J-dependence of Raman cross-section for the given vibrational band of the H_2 molecule transitions [17, 18].

In the limiting case of wide and smooth spectral profiles of the engaged pump lasers (with the spectra widths $\gg \Gamma_J$), neglecting the neighboring line wings, we may assume that when collisional broadening exceeds Doppler broadening, the relation $S(\Gamma_J) \propto 1/\Gamma_J$ [16] is valid, and the integral intensities of the CARS spectral lines can be written in the form

$$I_J = \mathrm{const}(N\Delta\rho_J)^2\left(\frac{d\sigma}{d\Omega}\right)_J\frac{1}{\Gamma_J}. \tag{3}$$

Thus, at the efficient overlapping of the broad spectra of the pump lasers with the lines of the Raman-active transitions, the registered integral intensities of the ^{0-1}Q-branch lines of the CARS spectrum in fact represent the populations, N_J, of the rota-

tional levels of the state with $\upsilon = 0$ at the given temperature, T, in dependence on their energy, E_J:

$$N_J(T) = \frac{N\Delta\rho_J}{1-\exp(-E_\upsilon/kT)} = N\frac{g_{ns}(2J+1)\exp(-E_J/kT)}{Z_R(T)(1-\exp(-E_\upsilon/kT))^{-1}}, \quad (4)$$

where $E_J/hc = -[BJ(J+1) - DJ^2(J+1)^2]/kT$; B and D are the rotational constants; g_{ns} and $g = g_{ns}(2J+1)$ are the nuclear spin and total degeneracy factors of the J-state, respectively; $Z_R(T)$ is the rotational partition function; $E_\upsilon = 4161$ cm^{-1} is the vibrational energy of H_2 molecules in the $\upsilon = 1$ state; k is the Boltzmann constant.

From (3) and (4), it follows that the dependence of the $Y_J = \ln\left((I_J\Gamma_J/(d\sigma/d\Omega)_J)^{1/2}/(2J+1)\right)$ values (a derivative from the measured intensities) on the energies, E_J, of the rotational levels of the $\upsilon = 0$ state is linear. Thus, we determined the temperature values from each spectrum from the tangent of the slope angle of the $Y_J(E_J)$ straight line calculated by means of the least-squares technique. Here, as we noted above, we take into account only the strongest components of the ^{0-1}Q-branch with odd J ($^{0-1}Q_3$—$^{0-1}Q_9$).

As the temperatures in the premixed flame of the McKenna burner were rather high (1400–1900 K), and the gas densities were relatively low ((4–5) × 10^{18} mol/cm^3), when determining the temperature from the CARS spectra, we considered the lines of the ^{0-1}Q-branch to be inhomogeneously broadened due to the Doppler effect, with minor influence of Dicke narrowing [19] and of collisional broadening by the surrounding molecules, that is, predominantly by N_2 and H_2O [20]. Doppler line widths are in fact the same for all the registered ^{0-1}Q-branch lines, while collisional effects are responsible for the occurrence of their width dependence on the quantum number, J. Yet, at low densities, the integral intensities of the lines, I_J, in the dual broadband CARS spectrum, after the nonresonant background subtraction (if present) can be, with a good accuracy, assumed to be independent of their width and to be proportional to the square of the population, N_J, of the lower levels of the respective transitions.

The accuracy of temperature values obtained from single-shot dual broadband CARS spectra of H_2 within the range of 1400–1900 K when analyzing a series of 300 spectra (the relative mean-square deviation, σ_H) was 3–5% [9]. The σ_H value turned to be in fact independent of the mass flow rates of the components, at the given stoichiometry, Φ, and insufficiently decreased with the Φ increase, possibly, due to the better mixing of the fuel with the oxidizer.

Two contributions exist into the mean-square deviation value, σ_H: the first, σ_I, originates from the "instrumental" measurement error, while the second, σ_T, is determined by the actual instability of the local temperature in the flame. On the base of the calibration results of the McKenna burner flame thermometry, at different mass flow rates of the components and different mixture stoichiometries [9], we might take $\sigma_I \approx 4\%$ in our case.

RESULTS

Spectra in the High Pressure Burner

We registered the CARS spectra of H_2 and H_2O molecules in several spatial points inside the combustion chamber, at different total mass flow rates, within the pressure range $P = 0.1$–2.1 MPa and within the stoichiometry range $\Phi = 0.5$–2.5. Figures 2 and 3 show the examples of the CARS spectra registered in the burner flame during a single laser shot and normalized by the nonresonant CARS spectrum. Up to the maximal implemented pressures, at the high temperatures, $T = 2000$–3000 K, in the H_2 molecule spectra within the range of 3780–4170 cm^{-1} (Fig. 2) we observe narrow lines of the ^{0-1}Q-branch up to $J = 11$ (the J values are given in the figure near the lines) and a number of the "hot" ^{1-2}Q-branch transitions. The nonresonant background in the spectra is relatively low. The CARS spectra (acquired with polarization suppression of the nonresonant background) of the $\nu_1 = 3652$ cm^{-1} vibrational band of H_2O molecule within the range of 3400–3700 cm^{-1} have a complicated rotational structure of the Q-branch, and in heated gas and at elevated pressures look like poorely structured broad bands (Fig. 3). Their shape strongly depends on temperature. In the fuel-rich mixture, the lines of the $^{0-1}O_3$ and $^{1-2}Q_9$ transitions of H_2 molecules, overlapped with this band, are clearly seen (see the spectrum a in Fig. 3). In

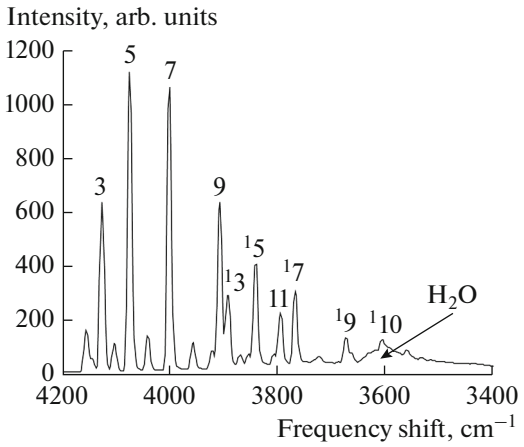

Fig. 2. CARS spectrum of H_2 molecules in the burner flame at the pressure of 0.9 MPa and the temperature ~3000 K; $X = -2$ mm, $Z = 1$ mm: the numbers with the superscript "1" are the rotational quantum numbers, J, of the ^{1-2}Q-branch lines.

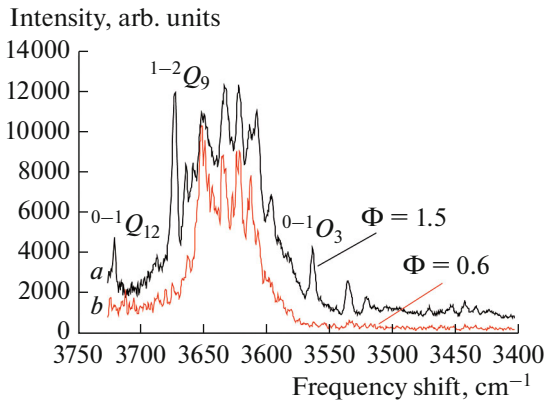

Fig. 3. CARS spectra in the turbulent flame of the burner with the single injector ($X = -2$ mm, $Z = 16$ mm) in the range of the ν_1 vibration Q-branch of H_2O molecules.

that case, the ratio of the integral line intensities of H_2 and H_2O molecules might serve as a characteristic of combustion efficiency.

As the integral intensity of the H_2O Q-branch and of the overlapping H_2 lines is much lower than that of the strongest lines of the H_2 ^{0-1}Q-branch, significant nonresonant background was often observed in the H_2O spectra. Because of that, sometimes we acquired the spectra with polarization suppression of the nonresonant background [5–7] in order to improve the contrast, and sometimes we did it without such suppression. In the first case, the background intensity was suppressed by more than 250 times whereas the H_2O band intensity decreased by only about seven times.

Temperature Determination from the CARS Spectra of the H_2 Molecules

We determined the gas temperature using the integral intensities of the $^{0-1}Q_3$–$^{0-1}Q_{11}$ lines of H_2 molecules after subtracting the low-level nonresonant background, as it is described above in relation to the calibration measurements at atmospheric pressure. But at elevated gas pressures typical for our experiments ($P \geq 0.6$ MPa), the spectral lines are homogeneously broadened by collisions, with the widths of the form $\Gamma_J = (4\pi D_0 \nu_J^2/cN) + \gamma_J N$ where D_0 is the diffusion coefficient; ν_J is the transition frequency; and γ_J is the collisional broadening coefficient dependent on the local composition and temperature of the gas, surrounding H_2 molecules. Here, the line intensities are still related to the level population by the expression (3). In the considered situation, for correct temperature determination from the integral intensities of the H_2 lines, the knowledge of the J-dependence of those line widths [19–22] is important. This dependence occurs at rather high pressures and is different for different H_2 collision partners. The main contribution into the broadening of the H_2 lines in the flame is given by H_2O molecules: the broadening coefficients for H_2O molecules are noticeably higher than those for H_2, O_2, and N_2 [21, 22]. Moreover, in the H_2/O_2 flames with $\Phi = 0.9$–2.5, typical for our experiments, H_2O molecules are the predominant component [23].

The qualitative estimates of the line width values on the base of the data available [21, 22] show that the collisional broadening of the H_2 lines by H_2O molecules (at $P = 1.1$ MPa and $T = 3000$ K) might vary from ~0.15 cm^{-1} ($^{0-1}Q_1$) to ~0.08 cm^{-1} ($^{0-1}Q_5$), while Doppler line widths are ~0.14 cm^{-1} (here everywhere the values are given of the full line width at half-maximum – FWHM). Thus, when determining the relative populations from the integral line intensities, one should account for the differences in the transition line widths, in spite of the fact that, according to the data on broadening coefficients by different gases, the J-dependence of the line widths becomes weaker with the temperature increase [21, 22]. In the present calculations temperature values initially obtained from the spectra without the account for the J-dependence of the line widths, were corrected if necessary (depending on the estimate of the local number density), with the help of the known parameters [21] of the temperature dependence of collisional broadening coefficients, $\gamma_J = \gamma_{J0}^{H_2-H_2O} + \tilde{\gamma}_{J0}^{H_2-H_2O} T$, of the H_2 lines by H_2O molecules. The number density of the latter was taken to be equal to the total number density of the molecules in the gas.

Note that the line intensities in the obtained spectra are well described by the Boltzmann distribution. This indirectly indicates to the fact that the characteristic size of spatial inhomogeneities in the investigated flame was larger than that of the probe volume, in contrast, say, to the situation we described in [4].

The transversal temperature profiles determined from 20 laser shot-averaged H_2 CARS spectra in the X–Z plane (that is, $Y = 0$ plane), which contains the axis of the central burner injector, were measured at different pressures in the chamber, at stoichiometry $\Phi \approx 1.0$ (mass flow rates were 32.3 slpm (standard liters per minute) for H_2, and 16.7 slpm – for O_2), and at different distances, Z, from the surface of the cooled plate with the injector matrix. The examples of the measured temperature distributions are shown in Figs. 4a ($P = 0.1$ MPa) and 4b ($P = 0.9$ MPa). Here, we blocked a part of the O_2 feeding channels at the distance of 2.5 mm from the burner axis in order to investigate the possibility to observe the local spatial nonuniformities in the temperature distribution and to estimate the actual spatial resolution in course of temperature measurements.

From the results of temperature profile measurements shown in Fig. 4, at the pressures of 0.1 MPa and 0.9 MPa, and at different distances from the injection plane, we see that the temperature at the flame axis

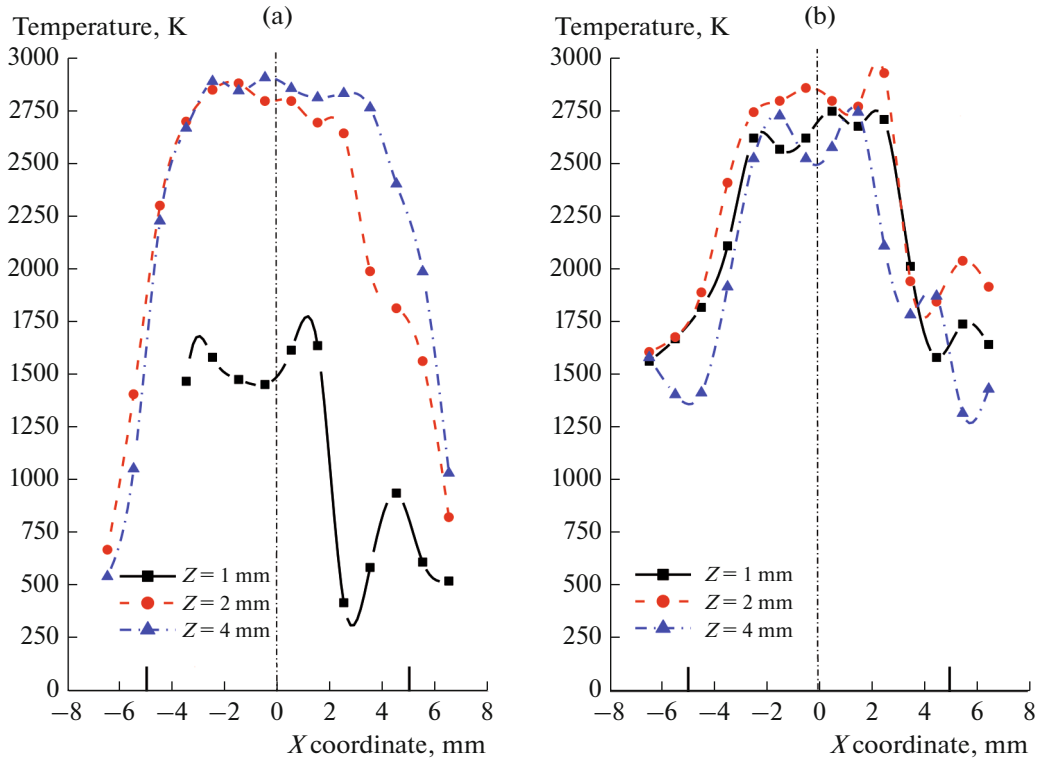

Fig. 4. Transversal temperature profiles at different distances from the injection plane: the vertical lines on the abscissa axis indicate the injector matrix boundaries: (a) 0.1, (b) 0.9 MPa.

reaches ~2800–2900 K and decreases to 600 K to the torch boundaries at $P = 0.1$ MPa and to 1500 K at $P = 0.9$ MPa. The plots explicitly show the temperature "dip" in the underheated H_2 jets near the blocked O_2 injectors, especially evident at $P = 0.1$ MPa near the surface of the plate with the injectors (at $Z = 1$ mm).

H_2 molecules are not present in the whole combustion volume, in particular, when burning lean mixtures. Meanwhile, H_2O molecules – the combustion products – do not decompose even at high temperatures. Thus, for local temperature measurements, of interest is to use calculated shape of the H_2O molecule spectra, further comparing them with those calculated at known gas pressure. Such calculations, especially if they take into account the interference with noticeable nonresonant background and with overlapping H_2 lines, present certain difficulties. In particular, the frequencies and the strengths of the lines of many H_2O molecule transitions from the states with high J values, populated at high temperatures, are unknown and not included into databases, thus giving no opportunity to simulate the shape of the spectrum (see Fig. 3) in the range of 3600 cm^{-1} with sufficient accuracy. As a result, this leads to lower measurement accuracy at high temperatures. In the present work, we did not perform such calculations. Earlier, in [24], we paid special attention to comparison of the local temperatures obtained from the H_2 and H_2O spectra in a similar flame.

Accuracy of Temperature Measurements and Temperature Fluctuations

The software developed to evaluate the temperatures from the integral intensities of H_2 spectrum lines obtained within a single laser pulse was automatically processing the series of 1000 spectra. If it appeared that line intensities in a spectrum were too low or too high and/or if the laser spark was detected, then this spectrum was discarded. In the predominant number of the processed series, the number of discarded spectra was within 1% and the peak intensity fluctuations from one spectrum to another were within the range of 500–10000 photodetector counts, while photodetector saturation level was 15000 counts and the noise level was only ~20–30 counts.

The temperature measurement accuracy is of a special interest, since the nonlinear character of the laser beam interaction in the turbulent medium causes essential fluctuations of the integral intensities of the spectral lines that are used for temperature determination. Two factors are the main cause of line intensity fluctuations. The first one is the laser beam power fluctuations which result in the intensity variation of the spectrum as a whole and do not perturb the relation between the particular line intensities. Thus, these

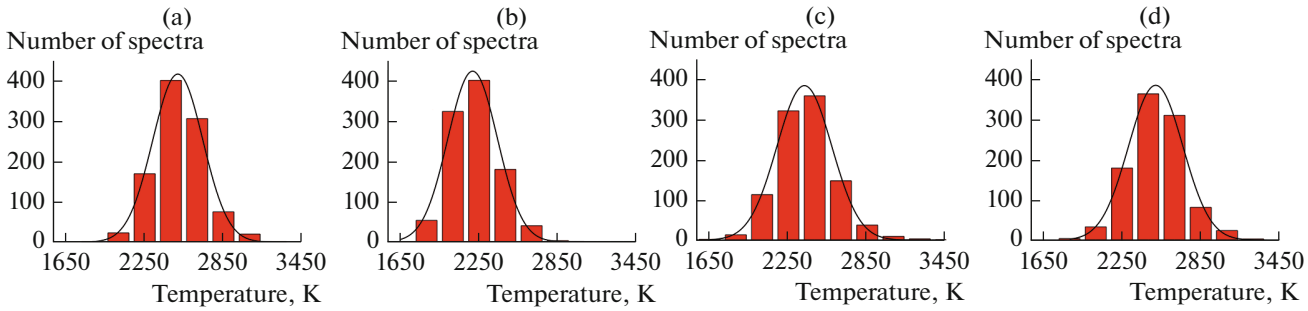

Fig. 5. Histograms of the gas temperature distributions at the pressures: (a) 0.5 MPa; (b) 0.7 MPa; (c) 1.2 MPa; (d) 1.7 MPa. In that point, the average temperature change with pressure rise is non-monotonous due to variations of the flame size and shape.

fluctuations do not cause occurrence of the "instrumental" errors in the temperature determination if the signal intensity falls within the dynamic range of the photodetector.

Another factor which, on the contrary, results in the "instrumental" errors in the temperature measurements is caused by random fluctuations of the spectral profile and/or of the phase distribution in the radiation of the dye lasers. Such fluctuations are immanently inherent in the laser emission and are unavoidable, although the studies aimed at minimization of the dye laser spectrum fluctuations were performed [25]. Use of the dual broadband pump in CARS provides a partial averaging of those fluctuations, making it possible to reduce their influence and to minimize the temperature measurement error.

To reveal which of the above factors dominates, the data processing software was calculating a sampling pair correlation coefficient, r_{3-7}, of the integral ${}^{1-0}Q_3$ and ${}^{1-0}Q_7$ line intensities in the measurement series at the given conditions

$$r_{3-7} = \frac{\mathrm{M}(I_3 I_7) - \mathrm{M}(I_3)\mathrm{M}(I_7)}{\sqrt{\left[\mathrm{M}(I_3^2) - \mathrm{M}^2(I_3)\right]\left[\mathrm{M}(I_7^2) - \mathrm{M}^2(I_7)\right]}}, \quad (5)$$

where $M(Y)$ is the mathematical expectation of the Y value. The selected lines are distinctly spaced in frequency, and the correlation of their intensity (or its absence) might be an evidence of the absence (or the presence) of fluctuations of the pump lasers spectral profiles. The r_{3-7} coefficient value gives an idea on which of the above factors is the governing for the intensity fluctuations in the CARS spectra. The low r_{3-7} values indicate to sufficient fluctuations of the ratio of the particular spectral line intensities and thus noticeable "instrumental" contribution into the scatter of the obtained temperature values. To the contrary, high (~1) r_{3-7} values promise a good accuracy of the thermometry. In the latter case, large variations of the obtained temperature values from one shot to another indicate to the local temperature fluctuations rather than to the measurement errors.

Figure 5 shows the histograms of the distributions of the gas temperatures measured during a single laser shot within the H_2/O_2 mixture combustion volume. The histograms correspond to the series of 1000 spectra obtained in one and the same flame point of the single coaxial injector burner ($X = -2$ mm, $Z = 16$ mm) near its Z axis (the X–Y plane, or $Z = 0$ plane, lies in the plane of the injection). The histograms are obtained at different pressures and at the mixture stoichiometry $\Phi \approx 0.6$ (the mass flow rate for H_2 is 19.8 slpm, and for O_2 – 17.1 slpm). The histograms clearly illustrate the scatter of the obtained values. The temperature distributions for all the performed measurement series are normal with a good accuracy. This is an evidence of the fact that the temperature scatter from one shot to another is of purely random nature.

The parameters of the normal distributions approximating the shape of the presented histograms (solid lines in Fig. 5), namely, the average temperature, T_H, and the mean-square deviation, δT_H, as well as of the relative mean-square deviation, σ_H, and the calculated coefficients, r_{3-7}, are presented in the Table. One can see that the temperature at the selected point (located sufficiently far from the injection plate) remains at about the same level (2200–2500 K), independently of the gas pressure in the burner (compare to Fig. 4). Here, we note that, with the pressure rise from 0.1 MPa to 0.5 MPa, the relative histogram width increases, thus indicating, with the simultaneous r_{3-7} coefficient growth, an increase in the temperature scatter in the given flame point. With the further pressure rise, the histogram width remains nearly constant. Note that with the pressure rise, the flame contracts and becomes more unstable and nonuniform, especially near the plane of injection.

Assuming the contributions into the histogram width from the single-shot "instrumental" measurement error , σ_I, and from the actual local temperature fluctuations in time in the turbulent medium, σ_T, to be statistically independent and taking the relative error of the temperature measurement from the spectra equal $\sigma_I = 4\%$, we might estimate the mean-square

Local average temperature, its statistical characteristics and correlation coefficient of integral line intensities in the flame

Pressure, MPa	Average temperature, T_H, K	Mean-square deviation of average temperature, δT_H, K	σ_H, %	Correlation coefficient, r_{3-7}	Mean-square deviation of temperature, δT, K	σ_T, %
0.1	2464 ± 3	155	4.7	0.51	59	2.4
0.5	2500 ± 3	192	7.7	0.88	164	6.5
0.7	2200 ± 8	188	8.5	0.89	166	7.6
1.2	2370 ± 3	208	8.3	0.89	185	7.8
1.7	2510 ± 5	207	8.3	0.92	181	7.2

σ_H, σ_T—the relative mean-square deviation of the temperature and of the average temperature, respectively.

relative value of the temperature scatter in the probe volume σ_T (see Table) during the whole measurement period (100 s) according to the relation $\sigma_T = \sqrt{\sigma_H^2 - \sigma_I^2}$. From the results presented in the Table, it follows that the temperature fluctuations with the typical temporal scale of 100 ms in the volume of $\varnothing 0.04 \times 2.5$ mm become actually measurable starting from the pressures of 0.5–0.6 MPa. Note that the increase of the correlation coefficient r_{3-7} with pressure is an evidence of the improved "instrumental" accuracy of the temperature measurements with the pressure rise (that is, the σ_I value decreases with pressure). Such a dependence is explained by the increase of the molecular transition line widths and thus by more efficient averaging of the spectral components of the pump lasers [9].

The presented discourse on the accuracy of the temperature measurements had only to do with the single-shot measurements, that is, during 10 ns. If only the measurements of the averaged temperature values are required, then the data from the Table are an evidence of the fact that the accuracy of such measurements for the time period of 100 s is 0.15–0.30%.

CONCLUSIONS

The present paper contains the results of application of broadband CARS spectroscopy in the conditions of turbulent combustion of H_2/O_2 mixtures at high pressures for:

—simultaneous acquisition of the rovibrational CARS spectra of H_2 and H_2O molecules in order to measure the local temperatures and to determine the combustion efficiency;

—measuring the fluctuations of the "instantaneous" local temperatures in dependence on pressure;

—obtaining the dependence of the characteristic peculiarities of combustion, such as spatial nonuniformities of the temperature field and of the flows in the gaseous component mixing zone, on the assigned mass flow rates of the fed fuel and oxidizer components, and on the operation pressure.

Using the dual broadband CARS spectroscopy, we determined the temperature and its temporal fluctuations at the pressures of 0.1–1.7 MPa within the range of 1000–3000 K with the error of a single (during 10 ns) measurement ~4%. The accuracy of the measurements of the averaged, during 100 s, temperature values in the quasi-stationary burning regime were as high as 0.15%. We performed the measurements of the spatial temperature distributions with the high resolution of about 0.04 mm in the transversal and 2.5 mm-in the longitudinal directions.

The performed measurements demonstrate the possibility of CARS to provide local diagnostics of gas mixtures at different sections of the gas-dynamic ducts of the perspective engines on the base of H_2/O_2 (or H_2-air) combustion; observations of the combustion process peculiarities depending on the pressure and the quantities of the fuel and oxidizer; studies of spatial nonuniformities of the reacting flows (cold zones, jets, shock waves) and of the process of gaseous component mixing; investigation of combustion in supersonic flows. The obtained data make it possible to compare the measurement results with the CFD-calculations and to test theoretical models of combustion.

ACKNOWLEDGMENTS

We are grateful to B.G. Sartakov for his help in the software modification and to the colleagues from the DLR Lampoldshausen: to W. Clauss, for preparation of the experiments; to D.N. Klimenko, for preparation of the experiments and participation in analysis of the experimental data; and to M. Oschwald, for fruitful discussions.

This work is partly supported by the Russian Foundation for Basic Research, project no. 14-08-00750-a and by the Presidium of the RAS, the Fundamental Research Program no. 46P.

REFERENCES

1. *Turbulent Mixing in Non-Reactive and Reactive Flows*, Murthy, S.N.B., Ed., New York: Plenum, 1975.
2. Favorskii, O.N. and Kurziner, R.I., *High Temp.*, 1990, vol. 28, no. 4, p. 606.

3. Bol'shov, M.A., Kuritsyn, Yu.A., Leonov, S.B., Liger, V.V., Mironenko, V.R., Savelkin, K.V., and Yarantsev, D.A., *Teplofiz. Vys. Temp.*, 2010, vol. 48, no. 1 (Suppl.), p. 9.
4. Vereschagin, K.A., Smirnov, V.V., Stel'makh, O.M., Fabelinsky, V.I., Sabelnikov, V.A., Ivanov, V.I., Clauss, W., and Oschwald, M., *Aerosp. Sci. Technol.*, 2001, vol. 5, p. 347.
5. Nibler, J.W. and Knighten, G.V., in *Raman Spectroscopy of Gases and Liquids*, vol. 11 of *Topics in Current Physics*, Weber, A., Ed., Berlin–Heidelberg: Springer, 1979, p. 253.
6. Greenhalgh, D.A., in *Advances in Nonlinear Spectroscopy*, vol. 15, Clark, R.J.H. and Hester, R.E., Eds., New York: Wiley, 1988, p. 193.
7. Eckbreth, A.C., *Laser Diagnostics for Combustion Temperature and Species*, New York: CRC, 1996, 2nd ed.
8. Kiefer, J. and Ewart, P., *Prog. Energy Combust. Sci.*, 2011, vol. 37, no. 5, p. 525.
9. Clauss, W., Fabelinsky, V.I., Kozlov, D.N., Smirnov, V.V., Stel'makh, O.M., and Vereschagin, K.A., *Appl. Phys. B: Lasers Opt.*, 2000, vol. 70, no. 1, p. 127.
10. Eckbreth, A.C. and Anderson, T.J., *Appl. Opt.*, 1985, vol. 24, no. 16, p. 2731.
11. Eckbreth, A.C. and Anderson, T.J., *Appl. Opt.*, 1986, vol. 25, no. 10, p. 1534.
12. Prucker, S., Meier, W., and Stricker, W., *Rev. Sci. Instrum.*, 1994, vol. 65, no. 9, p. 2908.
13. Bengtsson, P.-E., Martinsson, L., Alden, M., Lassesson, B., Johansson, B., Marforio, K., and Lundholm, G., in *Proc. 25th Int. Symp. on Combustion*, Pittsburgh, PA: Combustion Inst., 1994, p. 1735.
14. Bergmann, V. and Stricker, W., *Appl. Phys. B: Lasers Opt.*, 1995, vol. 61, no. 1, p. 49.
15. Hussong, J., Lückerath, R., Stricker, W., Bruet, X., Joubert, P., Bonamy, J., and Robert, D., *Appl. Phys. B: Lasers Opt.*, 2001, vol. 73, no. 2, p. 165.
16. Clauss, W., Kozlov, D.N., Pykhov, R.L., Smirnov, V.V., Stel'makh, O.M., and Vereschagin, K.A., *Appl. Phys. B: Lasers Opt.*, 1997, vol. 65, nos 4-5, p. 619.
17. Luthe, J.C., Beiting, E.J., and Yueh, F.Y., *Comput. Phys. Commun.*, 1986, vol. 42, no. 1, p. 73.
18. Marocco, M., *J. Raman Spectrosc.*, 2009, vol. 40, no. 7, p. 741.
19. Rahn, L.A., Farrow, R.L., and Rosasco, G.J., *Phys. Rev. A: At., Mol., Opt. Phys.*, 1991, vol. 43, no. 11, p. 6075.
20. Sinclair, P.M., Berger, J.Ph., Michaut, X., Saint-Loup, R., Chaux, R., and Berger, H., *Phys. Rev. A: At., Mol., Opt. Phys.*, 1996, vol. 54, no. 1, p. 402.
21. Michaut, X., Berger, J.-P., Saint-Loup, R., Chaussard, F., and Berger, H., in *Actes du Colloque de Synthese du Groupe de Recherche CNES/CNRS/ONERA/SNECMA. Combustion dans les Moteurs Fusees*, Toulouse: Cepadues Editions, 2001, p. 321.
22. Clauss, W., Klimenko, D.N., Oschwald, M., Vereschagin, K.A., Smirnov, V.V., Stel'makh, O.M., and Fabelinsky, V.I., *J. Raman Spectrosc.*, 2002, vol. 33, nos. 11–12, p. 906.
23. Gaseq. A Chemical Equilibrium Program for Windows. www.gaseq.co.uk.
24. Grisch, F., Vingert, L., Grenard, P., Fabelinsky, V., Vereschagin, K., and Oschwald, M., *Prog. Propul. Phys.*, 2013, vol. 4, p. 1051.
25. Snowdon, P., Skippon, S.M., and Ewart, P., *Appl. Opt.*, 1991, vol. 30, no. 9, p. 1008.

Translated by I. Dikhter